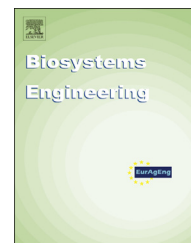


Available online at www.sciencedirect.com

SciVerse ScienceDirect

journal homepage: www.elsevier.com/locate/issn/15375110

Special Issue: Image Analysis in Agriculture

Research Paper

A new method for pedicel/peduncle detection and size assessment of grapevine berries and other fruits by image analysis[☆]



Sergio Cubero^{a,b}, María Paz Diago^{b,c}, José Blasco^a, Javier Tardáguila^b,
Borja Millán^b, Nuria Aleixos^{d,*}

^aCentro de Agroingeniería. Instituto Valenciano de Investigaciones Agrarias (IVIA). Cra. Moncada-Náquera km 5, 46113 Moncada, Valencia, Spain

^bInstituto de Ciencias de la Vid y del Vino (University of La Rioja, CSIC, Gobierno de La Rioja), 26006 Logroño, Spain

^cUniversità Cattolica del Sacro Cuore, Via Emilia Parmense 84, 29122, Piacenza, Italy

^dInstituto Interuniversitario de Investigación en Bioingeniería y Tecnología Orientada al Ser Humano. Universitat Politècnica de València. Camino de Vera s/n, 46022 Valencia, Spain

ARTICLE INFO

Article history:

Received 28 December 2012

Received in revised form

3 June 2013

Accepted 14 June 2013

The berry size of wine-grapes has often been considered to influence wine composition and quality, as it is related to the skin-to-pulp ratio of the berry and the concentration of skin-located compounds that play a key role in the wine quality. The size and weight of wine-grapes are usually measured by hand, making it a slow, tedious and inaccurate process. This paper focuses on two main objectives aimed at automating this process using image analysis: (1) to develop a fast and accurate method for detecting and removing the pedicel in images of berries, and (2) to accurately determine the size and weight of the berry. A method to detect the peduncle of fruits is presented based on a novel signature of the contour. This method has been developed specifically for grapevine berries, and was later extended and tested with an independent set of other fruits with different shapes and sizes such as peppers, pears, apples or mandarins. Using this approach, the system has been capable of correctly estimating the berry weight ($R^2 > 0.96$) and size ($R^2 > 0.97$) of wine-grapes and of assessing the size of other fruits like mandarins, apples, pears and red peppers ($R^2 > 0.93$). The proven performance of the image analysis methodology developed may be easily implemented in automated inspection systems to accurately estimate the weight of a wide range of fruits including wine-grapes. In this case, the implementation of this system on sorting tables after de-stemming may provide the winemaker with very useful information about the potential quality of the wine.

© 2013 IAGrE. Published by Elsevier Ltd. All rights reserved.

[☆] Developed from a presentation at the IV International Workshop on Computer Image Analysis in Agriculture, held at CIGR-AgEng 2012, Valencia, Spain: July 8th–12th, 2012.

* Corresponding author.

E-mail address: naleixos@dig.upv.es (N. Aleixos).

1537-5110/\$ – see front matter © 2013 IAGrE. Published by Elsevier Ltd. All rights reserved.

<http://dx.doi.org/10.1016/j.biosystemseng.2013.06.007>

1. Introduction

Machine vision systems are being used to automate inspection tasks in agriculture and food processing. Apart from its use in defect detection or colour estimation, image analysis is also an objective and reliable tool for examining other features such as shape and size (Cubero, Aleixos, Moltó, Gómez-Sanchis, & Blasco, 2011; Lorente et al., 2012).

Berry size and weight are two key parameters in the quality of table and wine-grapes. Berry size and weight parameters not only have an impact on the cluster architecture and compactness (leading to looser or tighter clusters), thereby influencing the cluster health status (Tardáguila, Martínez de Toda, Poni, & Diago, 2010), but are also considered indicators of grape and wine quality. In fact, berry weight and size, and their implications in grape and wine quality, have been extensively studied worldwide (Roby, Harbertson, Adams, & Matthews, 2004; Walker et al., 2005) and recently reviewed by Matthews and Nuzzo (2007). Most of the key compounds for wine quality, such as aromas and phenols, are located in the skin (Kennedy, 2010). Therefore, it is widely assumed that better wines are made from smaller berries, which have higher skin-to-pulp ratios (Barbagallo, Guidoni, & Hunter, 2011). Berry weight and size are common parameters for assessing wine-grapes' ripening from veraison to harvest (Iland, Bruer, Edwards, Weeks, & Wilkes, 2004) and quality features in table grapes. Their assessment – usually performed in the laboratory – often requires the removal of the berry pedicel, which is time and labour consuming.

Image analysis has recently been used outdoors to characterise several grapevine features, such as leaf area and yield (Diago et al., 2012). An important step forward would be the capacity to estimate berry size and weight from the analysis of images taken in the field, i.e. of the clusters hanging on the vines. This would allow close non-destructive monitoring of berry size throughout the ripening period of the actual clusters. In this respect, the detection of berry pedicels would be an even more critical step to avoid confounding effects.

The automatic detection of the pedicel in berries, or peduncle in other fruits (pedicel is normally used in the case of grain fruits that are joined together in a bunch and peduncle is more common for fruits joined directly to the branch of the plant), is still a challenge. Kapach, Barnea, Mairon, Edan, and Ben-Shahar (2012) offered an extensive description of the computer vision techniques that can be used for fruit-harvesting robots, concluding that the automation of some specific tasks is especially difficult, such as the detection of the peduncle in the grasping and picking operations carried out by the robot.

In some fruit, like oranges, the presence of large peduncles can damage other fruits during storage but their absence is considered a loss of quality. Sometimes it is important to detect the peduncle clearly in order to avoid confounding effects between the presence of the peduncle and external damage in automated quality inspection systems. If the peduncle is visibly different from the fruit, strategies based on colour information can be applied to locate it. Laykin, Alchanatis, Fallik, and Edan (2002) used colour information to discriminate between the peduncle on tomatoes and

bruises with a success rate of 100%. However, in other cases the difference between the peduncle and other defects is not so apparent. In these situations, Blasco, Aleixos, Gómez, and Moltó (2007) used visible images complemented by a multi-spectral system to discriminate among the peduncle and various defects in citrus fruits, achieving a peduncle identification rate of 67%.

Peduncle detection is also needed when information regarding the orientation of the fruit is required. Bennedsen and Peterson (2005) developed a computer vision system to detect defects in apples that had previously been oriented towards preventing the peduncles from appearing in the image. For the orientation process, these authors used a prototype developed by Throop, Aneshansley, Anger, and Peterson (2003), who oriented the apples with the peduncle on one side. In another work, Lu and Peng (2006) needed the fruit to be oriented with the end of the peduncle horizontal in order to obtain scattering measures in peaches. A similar idea was used by Blasco, Aleixos, and Moltó (2003), who acquired four images of apples from different views in order to estimate the size of the fruit in the image based on the equatorial diameter. For this purpose, the more perpendicular and centred the peduncle was, the better.

Harvesting robotics may also require peduncle detection systems to be implemented in order to collect the fruit properly. In this regard, Van Henten et al. (2006) presented a robotic system for de-leafing cucumber plants. To perform its tasks, the robot identified the pedicel of each leaf using two images at wavelengths of 850 nm and 970 nm, which can potentially be exported for use in actual harvesting robots. Hayashi et al. (2010) and Hayashi, Takahashi, Yamamoto, Saito, and Komeda (2011) used a machine vision unit based on three cameras installed on a robotic harvesting system to detect the position of strawberries and the orientation of the peduncle, thereby allowing accurate guidance of the robotic arm.

As can be seen, the detection of fruit peduncles is an important issue to be taken into account in the design of a computer vision system for estimating the quality features of fruit or vegetables. Several solutions have been proposed to determine the peduncle position, such as: the use of structured lighting to detect concavities in apples (Yang, 1993); colour segmentation techniques to differentiate the calyx and peduncle in citrus fruits (Ruiz, Moltó, Juste, Pla, & Valiente, 1996); or the study of light reflection in apples (Penman, 2002). In some of these works, the use of a spectral imaging system to locate the peduncle and discriminate it from other damage was required. Thus, the peduncles of some fruits present different reflectance values in the NIR region in relation to the skin of the fruit at certain wavelengths. Xing, Jancsó, and De Baerdemaeker (2007) used the texture of multispectral images to discriminate between smooth faces and those presenting peduncles in apples of different colours. A similar approach was taken by Nanyam, Choudhary, Gupta, and Paliwal (2012) to detect and discriminate the peduncle and leaves from defects in strawberries.

The main objective of this work was to develop an effective new method using image analysis and based on contour signatures to detect and remove the pedicel in images of grapevine berries using machine vision, and thus accurately

determine the weight and size (diameter) of grape berries. The algorithm was also tested with other fruits like mandarins, apples, pears, and so on to validate it.

This paper is organised as follows. In section 2 we present the materials and methods, including a description of the plant material, the vision system, the segmentation process and a detailed description of the peduncle/pedicle location algorithm. In section 3 we present the results obtained for the size and weight of grape berries, including the results for other fruits to validate the algorithm, as well as some discussion of the results. Finally, section 4 offers some conclusions from this work.

2. Materials and methods

The algorithms were developed and tuned using different images of 20 wine-grape berries of several colours and sizes, and captured with the pedicle at various random orientations. They were validated using another independent set of 100 single berries of different sizes and colours belonging to two grapevine (*Vitis vinifera* L.) cultivars (50 samples of Grenache and 50 of Tempranillo). The berries were placed on a white background inside a chamber equipped with a still camera (EOS 550D, Canon Inc, Japan) and four lamps each containing two fluorescent tubes (Osram L 18W/965 BIOLUX) with a colour temperature of 6500 K. The angle between the axis of the lens and the sources of illumination was approximately 45°, the insides of the inspection chamber were coated with anti-reflective material, and cross-polarisation was achieved by placing polarising filters in front of the lamps and in the camera lenses to minimise the impact of specular reflections produced on spherical fruits. The berries were oriented with the pedicle facing upwards and downwards interchangeably and the images were obtained with a size of 2592×1944 pixels and a resolution of $0.11 \text{ mm pixel}^{-1}$. The berries in the images included the pedicle, which makes it necessary to detect the insertion point between the fruit and the pedicle in order to obtain accurate measurements of the berry parameters. Two algorithms based on the radius function (Kunttu and Lepistö, 2007) and arc-length versus the turning angle graph (Wolfson, 1990) of the contour were developed to detect these points in the contour of the objects found in the images. In addition, a new algorithm based on a signature derived from these previous functions is proposed to improve the performance and robustness of a potential automatic system. To make the algorithm more robust and potentially general, the algorithms were also tested in other fruits like mandarins, pears, apples and peppers representing bigger spherical fruits, non-spherical fruits and irregular fruits with different types of peduncles and with randomly oriented peduncles.

For the manual assessment of grape berry size and weight, all imaged grape berries were individually labelled and weighed (XR20SSM-DR, Precisa Instruments Ltd., Switzerland), and their size was measured manually using an electronic calliper (Digital, TESLA SA, Switzerland) to determine the peduncle/pedicle–calyx (stem–calyx) axis and equatorial diameters. The resolution used for the size measurements was 0.01 mm. For the rest of the fruits tested to validate the peduncle/pedicle location algorithm, all the manual measurements for

determining the stem–calyx axis and the equatorial diameters were carried out using the same electronic calliper.

2.1. Segmentation and contour detection processes

Prior to the segmentation of images, an off-line process was carried out. This process consisted in generating a look-up table (LUT) that was later used to segment the images of the fruit. This process was performed using a computer application specially developed for this purpose that allowed an operator to select different windows in the images representing the background and peel/stem classes. The RGB values of the training windows selected were used as input in a Bayesian discriminant model (Harrel, 1991), the independent variables of the model thus being the grey levels of the RGB bands. Finally, the model was stored in a LUT which contains the classes of the model, and thus the segmented image contained the classes that each pixel belongs to. After image segmentation, a binary image showing the fruit in white and the background in black was obtained. The next step was to apply an algorithm which extracted the eight-connected contour by means of the chain code described by Freeman (1961).

2.2. Peduncle/pedicle location algorithm

One of the key points of the methodology presented here was the algorithm proposed to detect the connecting points between the peduncle and the fruit by analysing the contour of the fruit. Several approaches to analysing the contour of the objects have already been proposed for different purposes, like the analysis of the shape. Many of them propose the use of signatures, which are methods that represent a contour using a one-dimensional function. The best known is probably the radius signature (Blasco, Aleixos, Cubero, Gómez-Sanchis, & Moltó, 2009; ElMasry, Cubero, Moltó, & Blasco, 2012), which can yield a useful description of the shape of regular or manufactured objects with a known shape, but could fail when it is applied to biological objects with irregular or different shapes. Signatures are invariant against size or orientation, which makes them particularly interesting in cases where the size or the orientation of the object is unknown. Applied to peduncle detection, the main problem appears in irregular fruits, which present large variations in their signatures that make them unsuitable to identify the peduncle properly. Even in regular-shaped fruits this signature is sometimes not robust enough to ensure good results. A different descriptor of the perimeter is the curvature signature, although it has not been used frequently for food analysis but is common in other fields (Guliatto, de Carvalho, Rangayyan, & Santiago, 2008). Both of them have been tested in this work. The approach proposed in the present study was to obtain a new signature derived from the radius signature. This new signature analyses the changes in the direction of the curvature of the radius function. In regular fruits, these changes are supposed to be very smooth except when peduncle exists.

In the berries, the detection of the pedicle was carried out by an algorithm that consists in the following steps:

1. The centre of mass of the berry was calculated as the average coordinates of the pixels belonging to the fruit. A

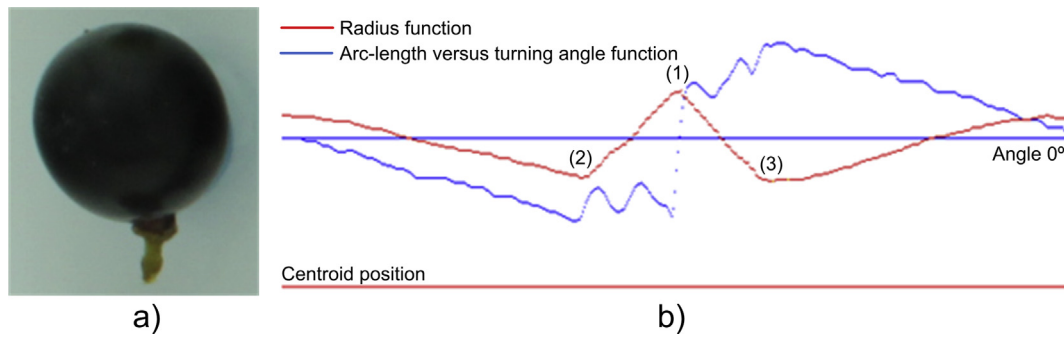


Fig. 1 – (a) Original image and contour of a grape berry with pedicel; and (b) its corresponding radius function and arc-length versus turning angle function.

faster method that could be used instead when the processing time is a constraint would involve using only the information about the boundary to estimate the centroid of the fruit. But in this case, the centroid could be too biased towards the pedicel/peduncle location if it is too long, and the performance of the method could decrease.

2. The radius function (Rubine, 1991) of the berry contour was calculated as a one-dimensional function in which each item of data was the Euclidean distance between the centroid and each of the points on the contour. This is represented in Fig. 1, where Fig. 1a shows a sample of the original image of a berry and the contour extracted with its centroid position. The radius function is shown in Fig. 1b. In this function it is supposed that the farthest point from the centroid corresponds to the top of the pedicel/peduncle and therefore the two local minima around this point are selected as the connecting points between the pedicel/peduncle and the fruit. The maximum value of the radius signature for the end of the pedicel/peduncle (1) and the

two contact points of the pedicel/peduncle with the berry (2), (3) can also be observed.

3. The second function calculated was based on the arc-length versus the turning angle graph of the curvature (Kalvin, Schonberg, Schwartz, & Sharir, 1986). In essence, the curvature consists in the rate of change of θ , the angle between the tangent vector to the curvature, and the horizontal axis for each point in the contour. The present work made use of the turning angle function (also called direction function), which consists in the graph showing the difference in θ at equally spaced points in the contour S_i ($i = 1 \dots n$), the difference being computed as reflected in Eq. (1) (Shih, 2010).
4. Finally, both functions were mixed to obtain a new one derived from the radius function that was thereafter called the radius direction signature. The new function was then obtained by applying the arc-length versus turning angle using the radius function as input instead of the fruit contour, which allows drastic changes in the outline of the

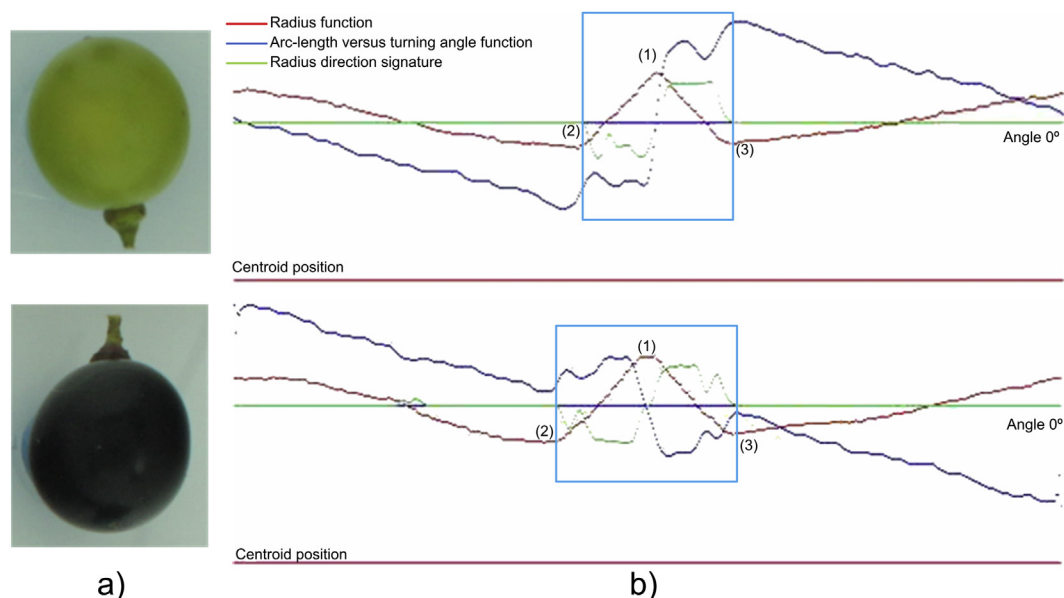


Fig. 2 – (a) Two samples of grape berries; and (b) their corresponding radius and arc-length versus turning angle function and radius direction signature.

fruits to be detected. This new function took values close to zero when the radius signature presented small changes, and different from zero otherwise.

$$\Delta\theta(S_i) = \theta(S_i + \Delta S) - \theta(S_i) \quad (1)$$

In this work ΔS was set to 4, which was enough to capture changes in the direction of the contour. Therefore, the Eq. (1) was modified as follows:

$$\Delta\theta(S_i) = \theta(S_{i-2}) - \theta(S_{i+2}) \quad (2)$$

For regular curves or shapes, the arc-length versus turning angle graph should be a monotonic decreasing function with values in the interval $[-\pi, +\pi]$ radians. When changes in the

contour are encountered due to irregular shapes or the presence of pedicel/peduncle, these are reflected on the graph of the function and can therefore be detected and analysed. An example of this signature is also shown in Fig. 1b for a berry with the pedicel oriented downwards.

Under the premise that the contour moves away from the centroid in the pedicel/peduncle part (the distance between the contour and the centroid increases), this new signature attempted to detect the points where these changes in the direction happened. In the case of spherical fruits, the distance from the contour to the centroid should be very similar for all points on the contour and therefore the function should present small changes. In a similar way, in the case of elliptical or other regular-shaped fruits, the changes should

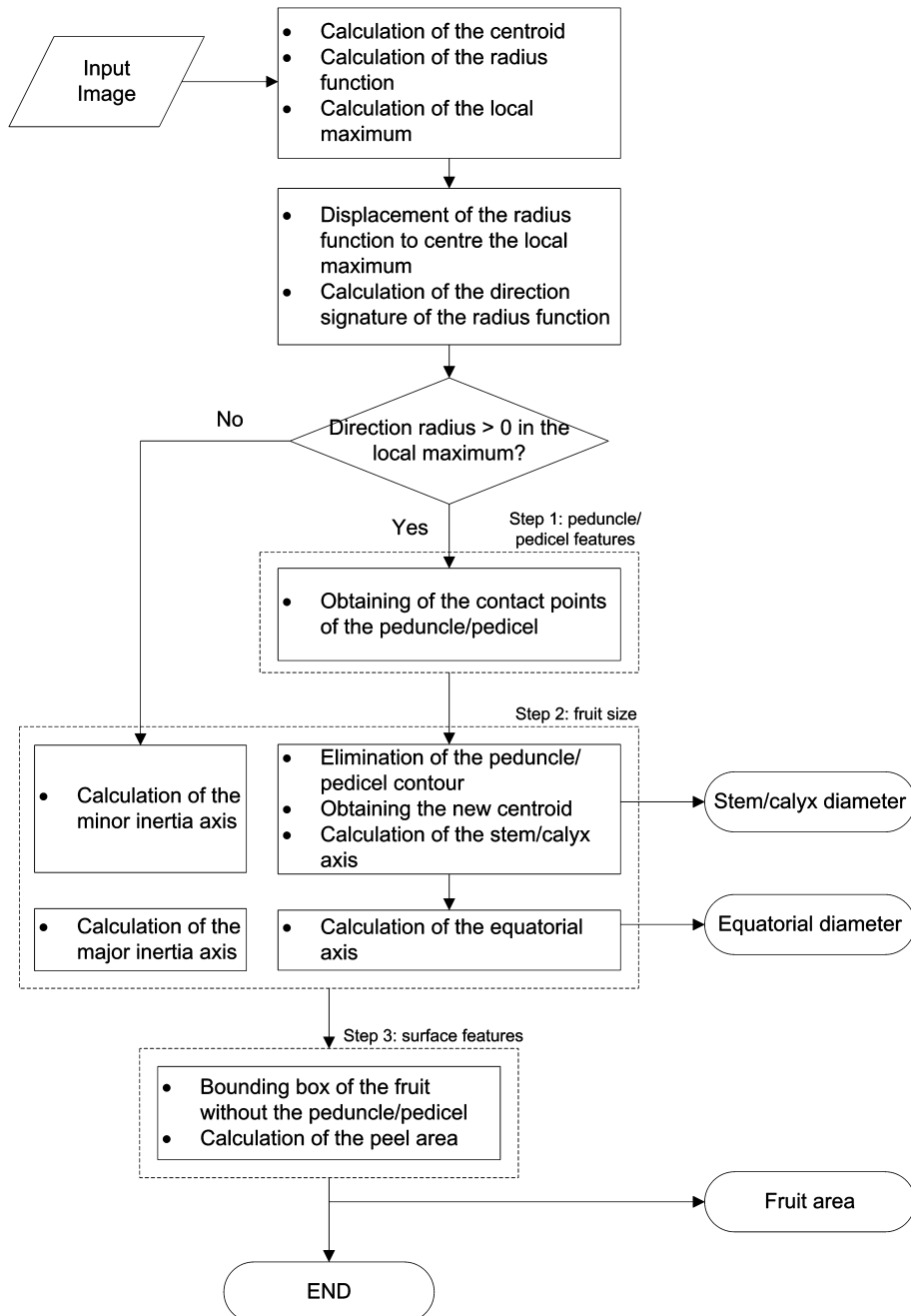


Fig. 3 – Flowchart for peduncle/pedicel detection and features extraction.

be smooth and constant. Figure 2 shows several samples of berries with different orientations of the pedicel (Fig. 2a) and their corresponding signatures (Fig. 2b). The local maximums have been centred in the graphs to make them easier to understand.

2.3. Validation process in grape berries

To estimate berry size, each individual berry was first located in the image and then the pedicel was detected following the algorithm described above. The two points identified as the connecting points between the pedicel and the fruit were joined to close the fruit contour while excluding the pedicel. Then, the centroid was calculated again without the influence of the pedicel and the size was estimated by means of the peduncle/pedicel axis and the diameter crossing the centroid, which was perpendicular to the previous peduncle/pedicel axis (equatorial diameter). The area of each berry was also estimated as the number of pixels belonging to the fruit

excluding the pedicel. The information about the area was used to predict the weight of each individual berry. The flowchart of the features extraction algorithm can be found in Fig. 3 and the pseudo-code of the main algorithm is presented in Fig. 4.

In order to assess the performance of the imaging system developed to predict the size (polar diameter) and weight of the berries in images including the pedicels, a regression model was built on a training set of 66 of the 100 berries. The remaining 34 berries were later used for validation.

2.4. Validation process in other fruits

To test the performance and robustness of the algorithm as well as its capability to be generalised to other fruits, a number of types of fruit with different shapes, sizes and colours were imaged in a variety of orientations and the images were processed to find the peduncles and size using the proposed approach. Particularly, a total of 30 pieces of

```

main () {

    Calculate the Radius_function of the contour;
    Search for the Maximum value in the Radius_function;
    Shift the contour so that the element corresponding to the Maximum in
        the Radius_function is centred;

    Calculate the Radius_function_new of the shifted contour;

    Calculate the Direction_function as the Arc-length versus the turning
        angle graph of the curvature;

    Calculate the Direction_Radius_function as the Arc-length versus the
        turning angle graph of the Direction_function;

    peduncle = false;
    for (i=0; i<total_points_contour; i++)
        if (Radius_Direction_function[i] != 0.0) {
            peduncle = true;
            break;
        }
    if (peduncle) {
        Search for the Local_minimum_1:
        for (i=0; i<total_points_contour/2; i++)
            if (Radius_Direction_function[i] != 0.0) {
                Local_minimum_1 = i; break;
            }
        Search for the Local_minimum_2:
        for (i=total_points_contour; i>total_points_contour/2; i--)
            if (Radius_Direction_function[i] != 0.0) {
                Local_minimum_2 = i; break;
            }
        Recalculate centroid without peduncle contour points;
        Remove peduncle contour points from original contour;
        fruit_size:
            Calculate stem/calyx diameter;
            Calculate equatorial diameter;
        fruit_weight = Calculate fruit_area;
    }
    else {
        fruit_size = Calculate inertia axes;
        fruit_weight = Calculate total_area;
    }
}

```

Fig. 4 – Pseudo-code of the algorithm for peduncle/pedicel detection.

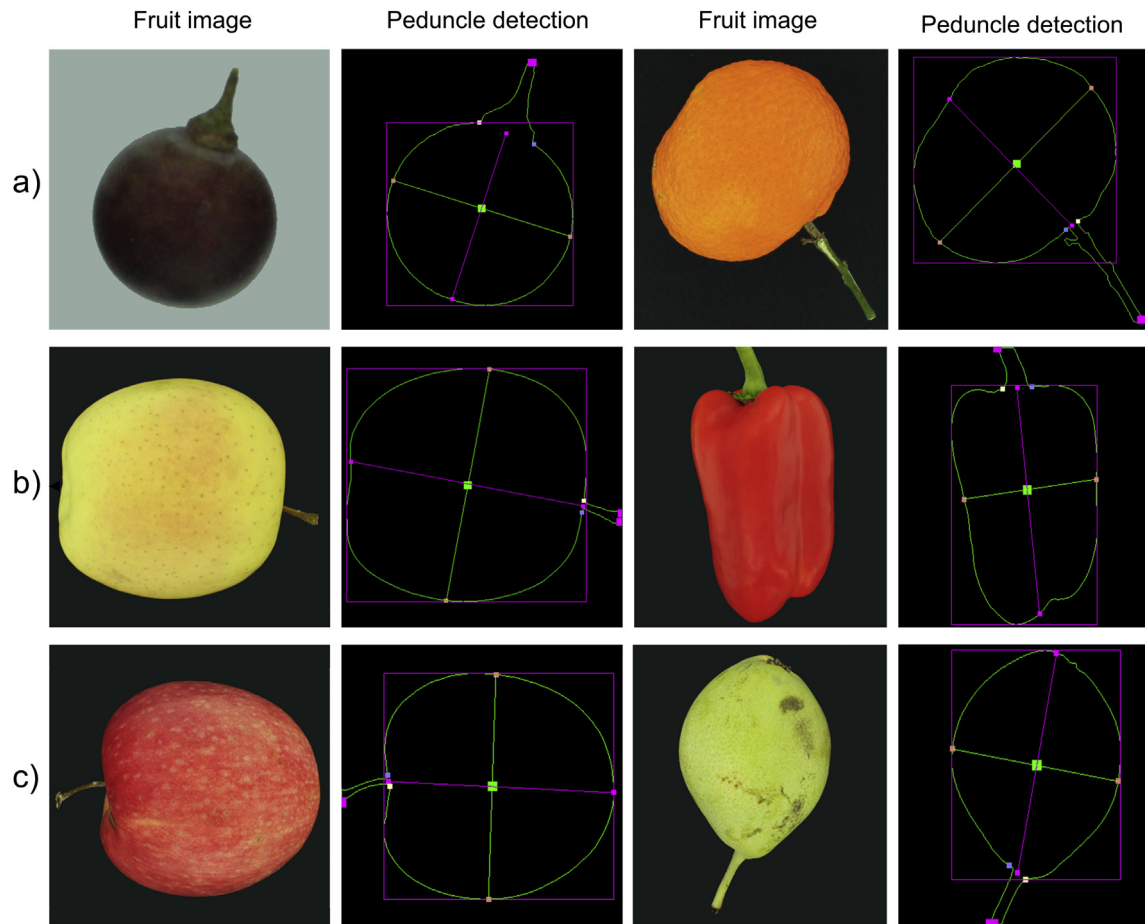


Fig. 5 – Results of peduncle detection and size estimation for some fruits tested with a random position of the peduncle: (a) for grape berry and mandarin, (b) for apple (“Golden Delicious”) and red pepper, and (c) for apple (“Royal Gala”) and pear.

each of these sets of fruits were used: pears cv. ‘Blanquilla’, apples cv. ‘Golden Delicious’ and cv. ‘Royal Gala’, red bell peppers cv. ‘Lamuyo’, and mandarins cv. ‘Nova’. For each set of different fruits, the peduncle was visible in the image for a total of 25 out of 30 fruits. The rest of the fruit had no peduncle or it was located inside the projected area of the

fruit. In the case of red peppers, all the samples contained peduncle. The size of this set was measured manually along the peduncle axis using a digital calliper and the measurements were recorded. The size of all the fruits was also estimated as the peduncle diameter from the closed contour of the fruit, excluding the peduncle.

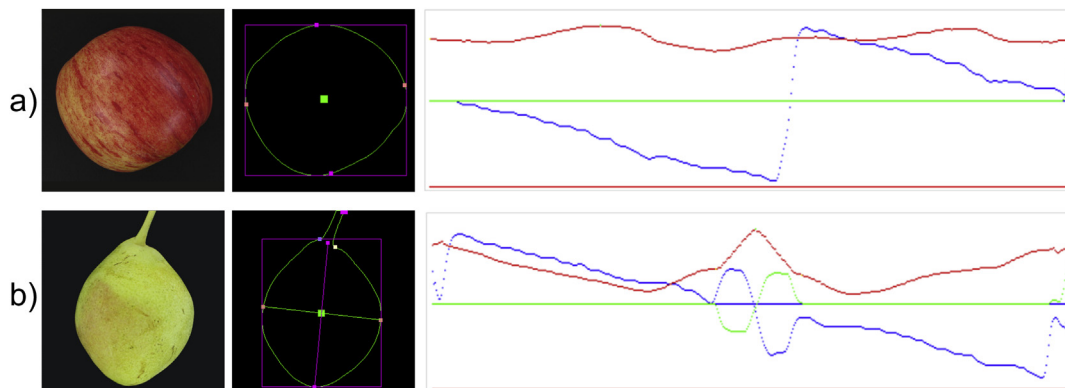


Fig. 6 – Example of results when (a) no peduncle was present in a ‘Royal Gala’ apple, compared to (b) a result with peduncle detected in a pear.

Table 1 – Regression analyses for the estimation of the size of ‘Grenache’ and ‘Tempranillo’ grape berries.

Grape variety	Parameter	Estimation	Std. error	T statistic	p-Value
Grenache	Constant	1.0436	0.2735	3.81	<0.001
	Polar diameter	0.9045	0.0198	45.76	<0.001
Tempranillo	Constant	0.8156	0.3350	2.44	<0.019
	Polar diameter	0.9086	0.0237	38.32	<0.001

Some of the results of the peduncle location algorithm for the fruits tested in this work are shown in Fig. 5. The points of contact between the peduncle and the fruit are depicted by small yellow and blue key points (small squares), and the base point of the peduncle is the midpoint in-between (pink key point). The distance between the base point of the peduncle and its opposite key point represents the diameter of the peduncle/pedicle, and the other two points on both sides of the centroid determine the length of the equatorial axis, both of which later correlated with the calliper measurements.

When no peduncle was present, the direction radius signature did not vary from zero since changes in the direction of the radius signature were very smooth, and both axes of inertia were calculated from the contour to obtain the size features. Figure 6 shows the differences in the signals calculated in images with and without peduncle.

3. Results and discussion

3.1. Assessment of grape berry size and weight by image analysis

Table 1 shows the statistical parameters for the regression model for the size estimation in ‘Grenache’ and ‘Tempranillo’ grape berries. The adjusted R^2 value obtained for the two grape varieties (0.97) confirmed the goodness of the linear regression found between the real and the estimated size values, the two coefficients being statistically significant (Table 1).

In order to validate the models properly, the next step was to use the regression models to predict the berry size values of the validation set. Figure 7 shows the validation results for both grapevine varieties. The validated R^2 values remained almost the same (a little bit lower, as expected for very high R^2

values), which finally gave rise to a reliable predictive model. This result indicates that the vision system developed for the estimation of the size of grape berries with pedicel was completely reliable and could be used as a useful laboratory tool replacing the very slow and tedious manual methods that are currently employed.

Similar analyses were performed to assess the goodness of the system at predicting the weight of individual berries obtaining a $R^2 = 0.98$ for cv. ‘Grenache’ and $R^2 = 0.96$ for the cv. ‘Tempranillo’ (Table 2) with p -value < 0.01 for both cultivars. To obtain more precise values of the weight, the pedicel was previously removed from the grape berries.

To validate the models, the regression models were used to predict the weight values of the validation set. Figure 8 shows the validation results for both varieties. These results indicated that the vision system developed was also reliable for estimating the weight of grape berries of both cultivars.

Berry size and weight are common parameters for monitoring grape maturity before harvest in the wine industry (Iland et al., 2004). Nevertheless, berry weight and size determination is conducted manually in the winery laboratory, and is therefore a tedious and time-consuming task. Cluster compactness, berry colour and health grape status are properties that are strongly influenced by berry weight (Tardaguila et al., 2010) and size.

On the other hand, berry size is also related to the skin-to-pulp ratio, which is widely assumed to be a grape and wine quality factor. Since the most decisive compounds for berry and wine quality, such as aromas and phenols, are located in the skin, the larger the skin-to-pulp ratio is, the higher the potential quality of the final wine will be (Barbagallo et al., 2011). Hence, smaller berries are often considered to yield better wines and are highly appreciated by winemakers, who usually include a grape berry separation step based on their

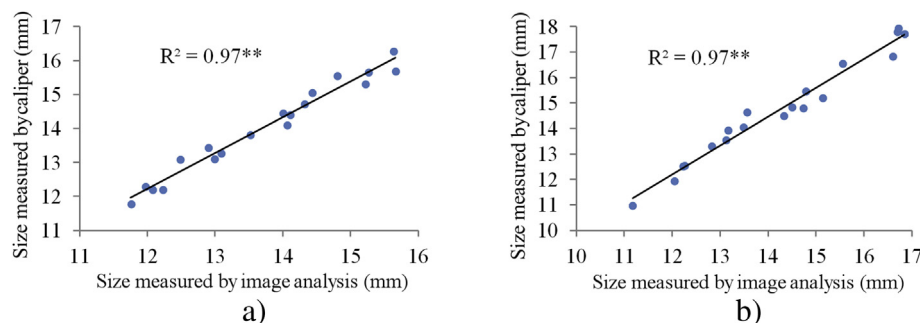


Fig. 7 – Adjustment to the linear model for the diameter of the berries from (a) ‘Grenache’, and (b) ‘Tempranillo’. Statistical significance at $p < 0.01$ is represented by ().**

Table 2 – Regression analyses for the estimation of the weight of ‘Grenache’ and ‘Tempranillo’ berries.

Variety	Parameter	Estimation	Std. error	T statistic	p-Value
Grenache	Constant	−0.6737	0.0566	−11.91	<0.001
	Weight-area	0.0148	0.0004	38.88	<0.001
Tempranillo	Constant	−0.6593	0.0524	−12.59	<0.001
	Weight-area	0.0149	0.0004	44.42	<0.001

size carried out on a sorting table when the intention is to produce high-quality wines.

Thus, the methodology developed for berry weight assessment, using image analysis, is a new, fast and inexpensive tool for the wine industry to monitor berry ripening and to evaluate potential grape and wine quality. This method could also be implemented as an inspection module on the sorting belts and tables of wineries producing high-quality ultra-premium wines, thereby replacing the manual separation based on berry size that is currently performed after the de-stemming process.

3.2. Detection of peduncle in other fruits

As stated in Section 2, the algorithm developed was also tested on other fruits, such as apples, pears, mandarins and peppers so as to be able to generalise it. The two functions and the signature described in Section 2.3 were used to detect the peduncle, and the best results were obtained for the new radius direction signature (Table 3), which includes the correct determination of all fruits without peduncle. The main drawback of using the radius signature was that minimum values did not always match the contact points of the peduncle with the fruit when this was non-spherical (because there were points closer to the centroid than the peduncle points). Furthermore, in irregular fruits the arc-length versus turning angle function showed sudden changes in different parts of the signal, which caused confusion with the peduncle.

Regarding the estimation of the fruit size, the peduncle/pedicle axis was compared to the manual calliper measurement, an adjusted $R^2 > 0.93$ being obtained for all types of fruit. This result confirmed the goodness of the regression, since p -value < 0.01 in all cases, thus demonstrating the reliability of the algorithms that were developed.

The limitations of the method mainly concerned the shape of the object, since the algorithm was able to determine the presence of the peduncle in regular and more or less rounded or compact fruits very well, but was not able to determine the presence or absence of the peduncle in fruits that were either elongated or that had irregular shapes, like the green peppers. This occurred because this method is based on the radius signature calculated as the distance of the contour points from the centre of mass. Therefore, although this centre was calculated from the area and not only from the contour, in elongated objects the centre of mass was biased to the peduncle (and sometimes outside the object surface), causing the local maximum of the polar signature to not always match the position of the end of the peduncle.

Another limitation concerns the requirement that the peduncle had to stand out from the contour of the object, which meant that the fruit or vegetable had to be oriented in order to image its profile, otherwise the peduncle could be detected, but not the correct size parameters. This can be observed in Fig. 9, where the detection of the peduncle is performed correctly (Fig. 9a), but the parameter of size is not (Fig. 9b). In contrast, the method performed well for regular-shaped fruits. This is important since it could potentially be applied in industrial imaging vision systems. For instance, Lefcourt et al. (2009) found that under particular loading conditions in industrial systems, rotating apples generally moved to an orientation where the peduncle/pedicle axis was parallel to the plane of the track and perpendicular to the direction of travel. This orientation would allow this algorithm to detect the peduncle location properly and to measure the size of the fruits accurately in real time, since the processing time needed to analyse one image is less than 40 ms. On the other hand, it could also be implemented in harvesting robots to orient or guide the robotic hand, but in

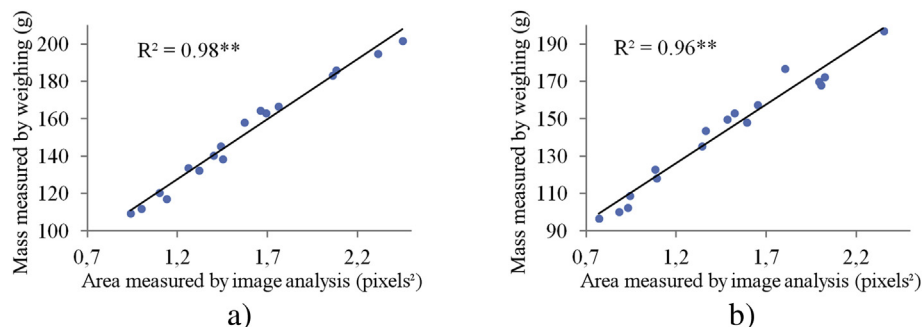
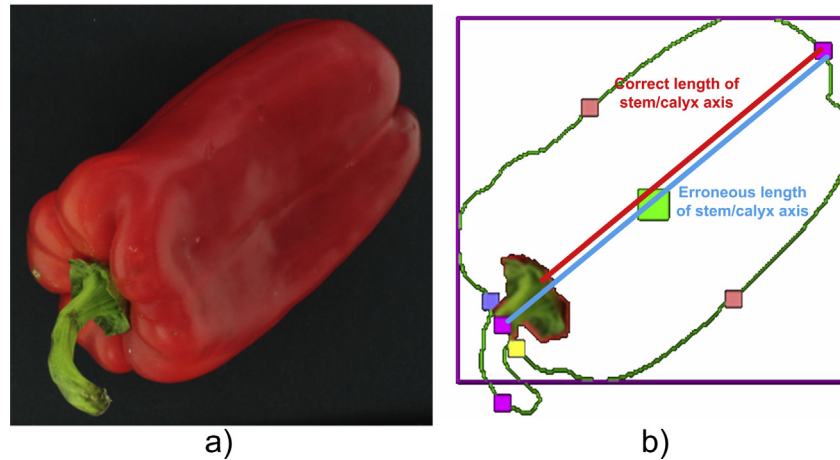


Fig. 8 – Adjustment to the linear model for the estimation of the weight of berries (a) ‘Grenache’, and (b) ‘Tempranillo’. Statistical significance at $p < 0.01$ is represented by ().**

Table 3 – Percentage of pedicel (grape berries) and peduncle (other fruits) detection using different signatures. For the coefficient of determination, R^2 was tested at $p < 0.01$.

Fruit	Radius function (%)	Arc-length vs. turning angle function (%)	Radius direction signature (%)	Size (R^2)
Grape berry	57.0	72.0	100	0.97
Mandarin	60.0	76.7	100	0.97
Apple Golden Delicious	50.0	63.3	96.7	0.96
Apple Royal Gala	40.0	60.0	96.7	0.96
Pear	16.7	60.0	96.7	0.96
Red pepper	20.0	30.0	90.0	0.93

**Fig. 9 – Example of result when the fruit was not well oriented on its profile and its impact on the size parameters.**

this case other problems related with the image segmentation could appear.

4. Conclusions

This work has presented a new, fast and inexpensive method to accurately assess the berry size and weight of wine-grapes, thus providing the wine industry with a cheap useful tool to monitor berry ripening and to evaluate potential grape and wine quality.

Moreover, a new effective method was developed to detect and remove the part of the peduncle/pedicel that protrudes from the fruit in the images taken by computer vision systems. The algorithm developed here could be applied to locate the peduncle/pedicel in order to have the fruit oriented or to avoid misclassification between the peduncle and defects, to accurately estimate the size while avoiding the effect of the peduncle, or also to measure the length of the peduncle. The new method does not require the segmentation of the peduncle and/or fruit defects in different regions, thereby allowing faster processing and can be used on standard images taken in the visible region of the spectrum. These two advantages make the proposed methodology faster and cheaper than other image vision methods that implement slow complex algorithms or require more expensive spectral computer vision equipment. The methodology developed here may be implemented in automated inspection systems

and robots for multiple purposes such as sorting or harvesting tasks.

Acknowledgements

This work has been partially funded by the Instituto Nacional de Investigación y Tecnología Agraria y Alimentaria de España (INIA) through research project RTA2012-00062-C04-01 and RTA2012-00062-C04-03 with the support of European FEDER funds, by the UPV-IVIA collaboration agreement through UPV-2013000005, and by UPV-SP10120276 Project.

REFERENCES

- Barbagallo, M. G., Guidoni, S., & Hunter, J. J. (2011). Berry size and qualitative characteristics of *Vitis vinifera* L. cv. Syrah. *South African Journal of Enology and Viticulture*, 32, 129–136.
- Bennedsen, B. S., & Peterson, D. L. (2005). Performance of a system for apple surface defect identification in near-infrared images. *Biosystems Engineering*, 90(4), 419–431.
- Blasco, J., Aleixos, N., Cubero, S., Gómez-Sanchis, J., & Molt, E. (2009). Automatic sorting of satsuma (*Citrus unshiu*) segments using computer vision and morphological features. *Computers and Electronics in Agriculture*, 66, 1–8.
- Blasco, J., Aleixos, N., Gómez, J., & Molt, E. (2007). Citrus sorting by identification of the most common defects using

- multispectral computer vision. *Journal of Food Engineering*, 83(3), 384–393.
- Blasco, J., Aleixos, N., & Moltó, E. (2003). Machine vision system for automatic quality grading of fruit. *Biosystems Engineering*, 85(4), 415–423.
- Cubero, S., Aleixos, N., Molt, E., Gómez-Sanchis, J., & Blasco, J. (2011). Advances in machine vision applications for automatic inspection and quality evaluation of fruits and vegetables. *Food and Bioprocess Technology*, 4(4), 487–504.
- Diago, M. P., Correa, C., Millan, B., Barreiro, P., Valero, C., & Tardáguila, J. (2012). Grapevine yield and leaf area estimation using supervised classification methodology on RGB images taken under field conditions. *Sensors*, 12, 16988–17006.
- ElMasry, G., Cubero, S., Molt, E., & Blasco, J. (2012). In-line sorting of irregular potatoes by using automated computer-based machine vision system. *Journal of Food Engineering*, 112, 60–68.
- Freeman, H. (1961). On the encoding of arbitrary geometric configurations. *IRE Transactions of Electronic Computers*, EC-10, 260–268.
- Guliatto, D., de Carvalho, J. D., Rangayyan, R. M., & Santiago, S. A. (2008). Feature extraction from a signature based on the turning angle function for the classification of breast tumors. *Journal of Digital Imaging*, 21(2), 129–144.
- Harrel, R.C. (1991). Processing of colour images with Bayesian discriminate analysis. International seminar on use of machine vision systems for the agricultural and bio-industries, Montpellier, France, pp 11–20.
- Hayashi, S., Shigematsu, K., Yamamoto, S., Kobayashi, K., Kohno, Y., Kamata, J., et al. (2010). Evaluation of a strawberry-harvesting robot in a field test. *Biosystems Engineering*, 105(2), 160–171.
- Hayashi, S., Takahashi, K., Yamamoto, S., Saito, S., & Komeda, T. (2011). Gentle handling of strawberries using a suction device. *Biosystems Engineering*, 109(4), 348–356.
- Iland, P., Bruer, N., Edwards, G., Weeks, S., & Wilkes, E. (2004). *Chemical analysis of grapes and wine: techniques and concepts*. Adelaide, Australia: Patrick Iland Wine Promotions Pty Ltd.
- Kalvin, A., Schonberg, E., Schwartz, J. T., & Sharir, M. (1986). Two-dimensional, model-based, boundary matching using footprints. *International Journal of Robotics Research*, 5(4), 38–55.
- Kapach, K., Barnea, E., Mairon, R., Edan, Y., & Ben-Shahar, O. (2012). Computer vision for fruit harvesting robots – state of the art and challenges ahead. *International Journal of Computational Vision and Robotics*, 3(1/2), 4–34.
- Kennedy, J. A. (2010). *Wine colour. Understanding and managing wine quality and safety* (pp. 73–104). Cambridge, United Kingdom: Woodhead Publishing.
- Kunttu, I., & Lepistö, L. (2007). Shape-based retrieval of industrial surface defects using angular radius Fourier descriptor. *IET Image Processing*, 1(2), 231–236.
- Laykin, S., Alchanatis, V., Fallik, E., & Edan, Y. (2002). Image processing, machine vision, tomatoes, classification. *Transactions of the ASABE*, 45(3), 851–858.
- Lefcourt, A. M., Narayanan, P., Tasch, U., Kim, M. S., Reese, D., Rostamian, R., et al. (2009). Orienting apples for imaging using their inertial properties and random apple loading. *Biosystems Engineering*, 104(1), 64–71.
- Lorente, D., Aleixos, N., Gómez-Sanchis, J., Cubero, S., García-Navarrete, O. L., & Blasco, J. (2012). Recent advances and applications of hyperspectral imaging for fruit and vegetable quality assessment. *Food and Bioprocess Technology*, 5(4), 1121–1142.
- Lu, R., & Peng, Y. (2006). Hyperspectral scattering for assessing peach fruit firmness. *Biosystems Engineering*, 93(2), 161–171.
- Matthews, M. A., & Nuzzo, V. (2007). Berry size and yield paradigms on grapes and wine quality. *Acta Horticulturae*, 754, 423–436.
- Nanyam, Y., Choudhary, R., Gupta, L., & Paliwal, J. (2012). A decision-fusion strategy for fruit quality inspection using hyperspectral imaging. *Biosystems Engineering*, 111(1), 118–125.
- Penman, D. W. (2002). Determination of stem and calyx location on apples using automatic visual inspection. *Computers and Electronics in Agriculture*, 33, 7–18.
- Roby, G., Harbertson, J. F., Adams, D. A., & Matthews, M. A. (2004). Berry size and vine water deficits as factors in winegrape composition: anthocyanins and tannins. *Australian Journal of Grape and Wine Research*, 10, 100–107.
- Rubine, D. (1991). Specifying gestures by example. *Computer Graphics*, 25(4), 329–337.
- Ruiz, L. A., Moltó, E., Juste, F., Pla, F., & Valiente, R. (1996). Location and characterization of the stem-calyx area on oranges by computer vision. *Journal of Agricultural Engineering Research*, 64, 165–172.
- Shih, F. Y. (2010). *Image processing and pattern recognition: fundamentals and techniques*. New Jersey, USA: John Wiley and Sons.
- Tardáguila, J., Martinez de Toda, F., Poni, S., & Diago, M. P. (2010). Impact of early leaf removal on yield and fruit and wine composition of *Vitis vinifera* L. Graciano and Carignan. *American Journal of Enology and Viticulture*, 61, 372–381.
- Throop, J.A., Aneshansley, D.J., Anger, W.C., & Peterson, D.L. (2003). Conveyor design for apple orientation. *ASAE Paper No. 03-6123*.
- Van Henten, E. J., Van Tuijl, B. A. J., Hoogakker, G.-J., Van Der Weerd, M. J., Hemming, J., Kornet, J. G., et al. (2006). An autonomous robot for de-leafing cucumber plants grown in a high-wire cultivation system. *Biosystems Engineering*, 94(3), 317–323.
- Walker, R. R., Blackmore, D. H., Clingeffer, P. R., Kerridge, G. H., Ruhl, E. H., & Nicholas, P. R. (2005). Shiraz berry size in relation to seed number and implications for juice and wine composition. *Australian Journal of Grape and Wine Research*, 11, 2–8.
- Wolfson, H. J. (1990). On curve matching. *IEEE Transactions on Pattern Analysis and Machine Intelligence*, 12(5), 483–489.
- Xing, J., Jancsó, P., & De Baerdemaeker, J. (2007). Stem-end/calyx identification on apples using contour analysis in multispectral images. *Biosystems Engineering*, 96(2), 231–237.
- Yang, Q. (1993). Finding stalk and calyx of apples using structured lighting. *Computers and Electronics in Agriculture*, 8, 31–42.